THE JOURNAL OF PHYSICAL CHEMISTRY Letters

Letter

pubs.acs.org/JPCL

Charge Transfer Dynamics from Organometal Halide Perovskite to Polymeric Hole Transport Materials in Hybrid Solar Cells

Jan C. Brauer,[†] Yong Hui Lee,[‡] Mohammad Khaja Nazeeruddin,[‡] and Natalie Banerji*[,†]

[†]Departement of Chemsitry, University of Fribourg, Chemin du Musée 9, CH-1700 Fribourg, Switzerland

[‡]Group for Molecular Engineering of Functional Materials, Institute of Chemical Sciences and Engineering, École Polytechnique Fédérale de Lausanne, CH-1015 Lausanne, Switzerland

Supporting Information

ABSTRACT: Organometal halide perovskites have emerged as promising next-generation solar cell technologies presenting outstanding efficiencies. However, many questions concerning their working principles remain to be answered. Here, we present a detailed study of hole transfer dynamics into polymeric hole transporting materials (HTMs), poly(triarylamine) (PTAA), poly(3-hexylthiophee-2,5-diyl (P3HT), and poly[2,6-(4,4-bis(2-ethylhexyl)-4*H*-cyclopenta[2,1-b;3,4-b′]dithiophene)-*alt*-4,7-(2,1,3-benzothiadiazole) (PCPDTBT). The hole transfer dynamics are shown to occur on a time scale of thousands of picoseconds, being orders of magnitude slower compared to hole transfer involving commonly used Spiro-OMeTAD as HTM.

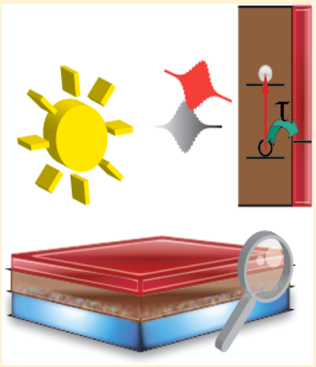

Organometal halide perovskites have created a surge of attention in the last couple of years due to their impressive performance as absorbers and charge transporters in photovoltaic and photoelectrochemical cells.[1−4] The main advantage of these materials is the combination of properties typically found in inorganic semiconductors, especially the high charge mobility, low exciton binding energy, and long diffusion length of charge carriers,[5,6] with the easy processability, band gap tunability,[7] and cost-effectiveness of organic materials. Significant efforts have been invested to optimize device architecture and material processing schemes in order to reach higher photovoltaic performance, stability, and reproducibility.[3,8,9] This has allowed an increase of the performance of perovskite solar cells from 3.8%[10] to certified efficiencies of over 20%.[11] The nature and evolution of the excited state, the mobility of the photogenerated charges, as well as the dynamics of initial charge transfer reactions to electron-transporting mesoporous TiO_2 scaffolds, or to hole transporting materials, typically Spiro-OMeTAD, have been investigated using time-resolved spectroscopy from the visible to the microwave spectral range.[12−14] Nevertheless, a thorough understanding of the initial fundamental processes occurring in those relatively young materials is still lacking and presents a challenge to researchers.

On the basis of the properties of the used perovskite, different designs for photovoltaic devices have been proposed including a mesoscopic TiO_2 structure,[15] a planar structure,[6,16] or even hole transporting material (HTM)-free cells.[17] It has become evident that the choice of the hole conductor (or hole transporting material, HTM), and the design of the HTM/perovskite interface, is of crucial importance for device efficiency. So far, the most studied and best performing devices contain Spiro-OMeTAD as HTM. Using Spiro-OMeTAD includes several drawbacks, such as its mostly empirically addressed need for complex doping and the high price. Therefore, efforts exist to replace Spiro-OMeTAD with alternative HTMs, for example conjugated polymers. Promising candidates include the polymeric hole conductors poly(triarylamine) (PTAA), poly(3-hexylthiophee-2,5-diyl (P3HT), and poly[2,6-(4,4-bis(2-ethylhexyl)-4*H*-cyclopenta-[2,1-b;3,4-b′]dithiophene)-*alt*-4,7-(2,1,3-benzothiadiazole) (PCPDTBT). In a recent study, Heo et al. systematically investigated the photovoltaic performance in devices containing those HTMs, and showed that PTAA can, under the used preparation conditions, outperform the molecular hole conductor Spiro-OMeTAD.[18] Here, we present the early charge transfer dynamics occurring in $TiO_2/CH_3NH_3PbI_3$/HTM systems with different polymeric HTMs, as obtained by ultrafast transient absorption spectroscopy (TAS). We have shown that hole transfer occurs efficiently for the investigated polymers, although the observed dynamics are orders of magnitude slower compared to time constants suggested for Spiro-OMeTAD.

Samples were prepared by a two-step deposition method of perovskite on a mesoporous TiO_2 layer[1,19] and covered by the HTM using spin coating. For the femtosecond-resolved TAS measurements, the samples were excited under inert atmosphere at various wavelengths in the visible range, and transient

Received: August 5, 2015
Accepted: September 2, 2015
Published: September 2, 2015

DOI: 10.1021/acs.jpclett.5b01698
J. Phys. Chem. Lett. 2015, 6, 3675−3681

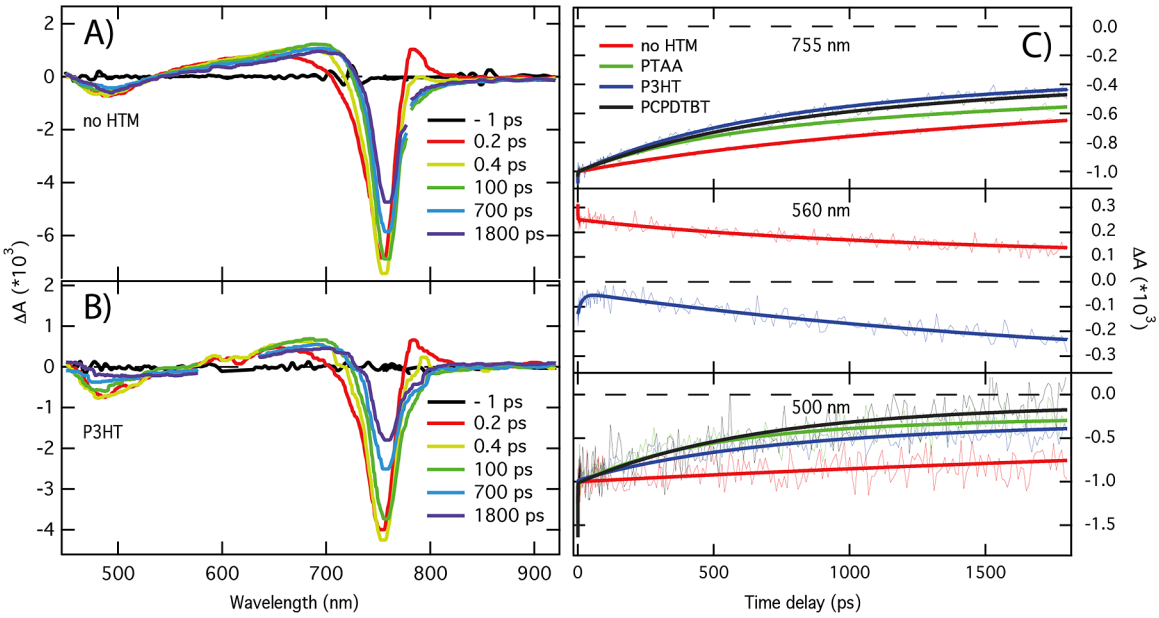

Figure 1. Transient absorption spectra following 600 nm excitation of (A) a $TiO_2/CH_3NH_3PbI_3$ sample (B) a $TiO_2/CH_3NH_3PbI_3$/P3HT sample (5−10 nm HTM thickness). Sometimes, the region around 600 nm was removed due to scattering by the pump excitation. C) TAS time profiles at probe wavelengths of 755, 560, and 500 nm for $TiO_2/CH_3NH_3PbI_3$, $TiO_2/CH_3NH_3PbI_3$/P3HT, $TiO_2/CH_3NH_3PbI_3$/PTAA and $TiO_2/CH_3NH_3PbI_3$/PCPDTBT samples. Solid lines represent the best multiexponential fit.

spectra were obtained with a white light probe. The experimental details can be found in the Supporting Information. In order to ensure that the experimental conditions yielded robust and reliable results, we verified that the obtained TAS dynamics were independent of irradiation conditions (backside/frontside illumination for thin HTMs, excitation fluence), substrate (glass with/without FTO), and thickness of the perovskite-coated mesoporous TiO_2 layer (Supporting Information Figure S4 and S5). To avoid any excitation-intensity effects, the data presented in the following were recorded at low fluence (<2.5 μJ cm^{-2} and <6.5 μJ cm^{-2} for 580−600 and 760 nm excitation, respectively).

The first set of investigated samples consists of $TiO_2/CH_3NH_3PbI_3$/HTM structures with a thin (5−10 nm) polymeric HTM capping layer compared to a sample lacking the HTM. Those correspond closely to the ones used by Heo et al. to obtain optimized solar cell efficiency.[18] TAS spectra and time profiles of the corresponding films excited at 600 nm are shown in Figure 1.

In the absence of the HTM, photoexcitation of $CH_3NH_3PbI_3$ leads to generation of excitons and charge carriers. The exciton binding energy in perovskite materials has been found to be close to 50 meV[20] and might be even as low as ∼2 meV,[21] indicating that at RT predominately free charges are generated. A significant portion of the electrons are injected into TiO_2 scaffold on the subpicosecond time scale.[13,22] In the TAS spectra without HTM (Figure 1A), two prominent negative bands are seen at ∼500 and 760 nm, as well as positive photoinduced absorption (PIA) bands at 530−720 and 790 nm. The positive bands contain information about the excited populations, about hot electrons and holes at early times and at later times about the evolution of excitons and thermalized charges.[22] A previous study attributed the two negative signals to bleaching transitions from two valence bands (VB1 and VB2) to a common conduction band (CB1)[14] due to depopulation of the valence band. Stamplecoskie et al. proposed the existence of a dual excited state composed of a charge transfer band at 480 nm and a charge separated state at 760 nm.[23] The fast (subpicosecond) spectral narrowing and red shift of the 760 nm band has been explained either by band filling effects following a Burnstein−Moss model[24] or by stimulated emission from thermally nonrelaxed states.[15,25]

The TAS spectra of the samples with thin polymeric HTMs (Figure 1, see also Supporting Information Figure S2 and S3) are also dominated by the spectral features of $CH_3NH_3PbI_3$. Figure 1C shows the TAS time profiles following 600 nm excitation probed at different wavelengths. The addition of a polymeric HTM to the $TiO_2/CH_3NH_3PbI_3$ layer induces slow quenching of both the 480 and 760 nm bands (i.e., faster decay compared to the sample without HTM), which is likely to be related to hole transfer from the excited $CH_3NH_3PbI_3$ to the HTM. As discussed above, the bands at 480 and 760 nm can be explained by a depopulation of VB1 and VB2 and a population of the CB, leading to reduced transition probabilities an therefore negative signals in the transient spectra. A hole transfer from the VBs of the photoexcited perovskite to the HTM would then lead to an increase of the population in the VBs and consequently to a decrease of the amplitudes of the bands at 480 and 760 nm. Surprisingly, this quenching occurs on a time scale of hundreds of picoseconds, which is much slower than the initial hole transfer observed using Spiro-MeOTAD as HTM.[15,22]

Given the ambiguous spectral assignment, and since an apparent change in the dynamics of the negative 480 and 760 nm bands might as well be explained by a modification of the surface energy landscape of the $CH_3NH_3PbI_3$ in the presence of the HTM, altering the charge carrier recombination rate within the perovskite, a more convincing prove of hole transfer would be the observation of the polymer's ground state bleaching (GSB) or polaron absorption following excitation of the $CH_3NH_3PbI_3$. Selectively exciting the perovskite in a perovskite/HTM system leads in a first step to a depopulation of the perovskite VBs and population of the conduction band, whereas the P3HT remains in its ground state. From this

DOI: 10.1021/acs.jpclett.5b01698
J. Phys. Chem. Lett. 2015, 6, 3675−3681

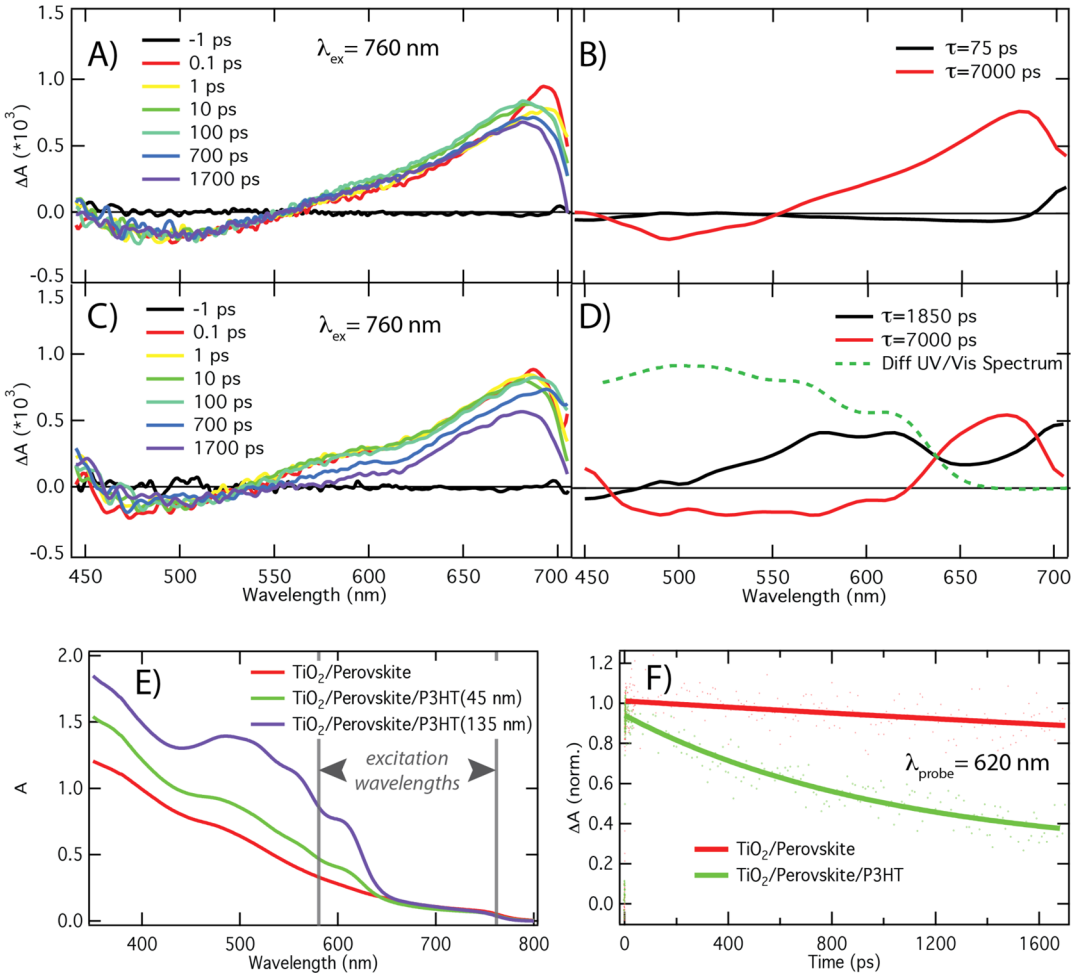

Figure 2. Transient absorption spectra upon excitation at 760 nm of (A) $TiO_2/CH_3NH_3PbI_3$ and (C) $TiO_2/CH_3NH_3PbI_3$/P3HT (45 nm). Decay-associated amplitude spectra resulting from the global analysis of the dynamics of (B) $TiO_2/CH_3NH_3PbI_3$ and (D) $TiO_2/CH_3NH_3PbI_3$ /P3HT. (E) Steady-state spectra and indication of the used excitation wavelengths. (F) Comparison of the dynamics upon excitation at 760 nm probing at 620 nm for $TiO_2/CH_3NH_3PbI_3$ and $TiO_2/CH_3NH_3PbI_3$/P3HT (45 nm).

state, three processes are conceivable: the electron and hole recombine within the perovskite, energy transfer from the photoexcited perovskite to the HTM, or hole transfer from the perovskite VB to the HTM. The first process does not affect the HTM, and therefore, no signature of a HTM GSB would occur. The second process would indeed lead to a GSB of the HTM, but would be energetically uphill in the case of P3HT. Therefore, we assign the emergence of a GSB of P3HT following selective excitation of the perovskite to a hole transfer reaction. In Figure 1, we observe a positive signal at around 560 nm for the $TiO_2/CH_3NH_3PbI_3$ sample (PIA of the perovskite), which becomes negative upon addition of P3HT, due to the overlapping bleaching of the polymer. This negative GSB is present at the shortest time delays suggesting some direct excitation of the P3HT at 600 nm, then weakly decays (see discussion below), and finally slowly rises again on a time scale of several hundred picoseconds (Figure 1C). By comparing the dynamics at 560 nm with the quenching of the negative bleaching and/or SE bands of $CH_3NH_3PbI_3$, it seems reasonable to attribute the rise of the polymer's GSB to an indirect ground state depletion caused by slow hole transfer from the photoexcited perovskite. However, the amplitude of the P3HT GSB signal in this sample is very small due to the thin layer of P3HT, so that a convincing data interpretation is not possible.

To confirm the initial results, a second set of samples that have different thicknesses of the P3HT layer was prepared. The corresponding steady-state absorption spectra are shown in Figure 2E, where the absorption of P3HT superposed to the absorption of $CH_3NH_3PbI_3$ is clearly visible. From the absorbance, the P3HT layer thickness was estimated to 45 nm for the thinner of the new samples.[26] To selectively excite the perovskite layer, we choose 760 nm as excitation wavelength this time. Because of the selective excitation of the perovskite, no direct observation of the P3HT GSB was expected. As outlined above, any emergence of the GSB of P3HT in this experiment would be an unambiguous signature of hole transfer, indirectly populating the polymer states. At early time delays, the transient spectra for both samples (without HTM and with the 45 nm P3HT layer) show the already discussed features of photoexcited perovskite with similar initial signal amplitude (Figure 2), confirming that at 760 nm excitation we do not excite P3HT directly and that no substantial hole transfer is occurring at time scales faster than the experimental time-resolution. By comparing the transient spectra with and without P3HT at longer times, we observe that the excited state absorption and the 480 nm bleaching

DOI: 10.1021/acs.jpclett.5b01698
J. Phys. Chem. Lett. 2015, 6, 3675−3681

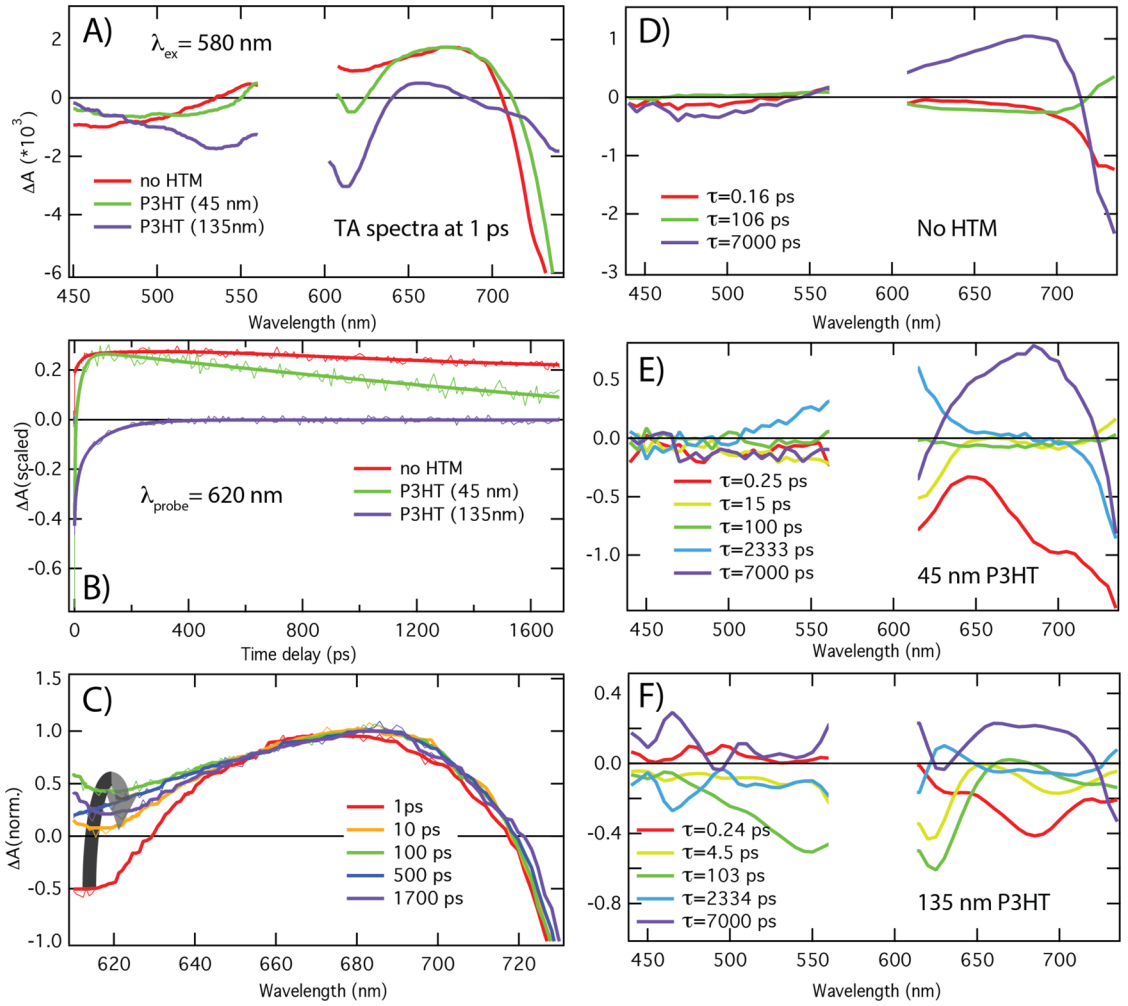

Figure 3. (A) Transient absorption spectra 1 ps after excitation at 580 nm of $TiO_2/CH_3NH_3PbI_3$, $TiO_2/CH_3NH_3PbI_3$/P3HT (45 nm) and $TiO_2/CH_3NH_3PbI_3$/P3HT (135 nm). (B) Corresponding dynamics at 620 nm. (C) Zoom into the normalized TA spectra of $TiO_2/CH_3NH_3PbI_3$/P3HT (45 nm) at various time delays after excitation at 580 nm. (D)−(F) Amplitude spectra resulting from the global analysis of the dynamics, for $TiO_2/CH_3NH_3PbI_3$, $TiO_2/CH_3NH_3PbI_3$/P3HT (45 nm), and $TiO_2/CH_3NH_3PbI_3$/P3HT (135 nm), respectively.

signal of the perovskite are quenched upon addition of P3HT, whereas the GSB of P3HT becomes visible at long time delays as an indent at 570 and 620 nm (Figure 2C). Figure 2F shows the time profiles probed at 620 nm, with and without the HTM. The faster decay within hundreds of picoseconds in the presence of P3HT, which is caused by both the decay of the excited state absorption and the rise of the polymer's GSB, is clearly visible.

To investigate the hole transfer reaction in more detail, multiexponential global analysis[27] of the TAS data has been performed and the results are shown in Figure 2B and D. In the global analysis procedure, the dynamics at all wavelengths are fitted simultaneously to a convolution of a Gaussian and the sum of two exponential functions. The amplitudes are allowed to vary freely for each wavelength, whereas the time constants are set to be the same for the whole spectral range (see Supporting Information for details). The traces shown in Figure 2B and D therefore indicate the spectral components that evolve with the same time constant. The results show that in the case of $TiO_2/CH_3NH_3PbI_3$, all spectral features evolve basically with one time constant of 7 ns, due to the slow recombination of the charge carriers and excitons within the perovskite. Minor spectral dynamics also occur within 75 ps; this rise of the positive band at 530−700 nm might be related to exciton formation.[22] In the case of $TiO_2/CH_3NH_3PbI_3$/P3HT, a component with a time constant of 1850 ps becomes important. The spectral shape of this component corresponds closely to the steady-state spectrum of the P3HT layer (dotted line in Figure 2D, obtained by taking the difference of UV/vis spectra of $TiO_2/CH_3NH_3PbI_3$ and $TiO_2/CH_3NH_3PbI_3$/P3HT) and therefore can be clearly attributed to a slow ingrowth of the GSB of P3HT. Because at 760 nm we selectively excite the perovskite (no direct P3HT excitation), we can assign the rise of the polymer's GSB to hole transfer from the excited perovskite to P3HT. The amplitude spectrum related to the 7 ns decay contains both signatures of the excited perovskite and of the GSB of P3HT, indicating long-lived charge separation.

In the above-mentioned experiment, we have excited the perovskite close to the band gap to avoid direct excitation of the P3HT at shorter wavelengths. It could be argued that the observed slow hole transfer (with a time constant of 1850 ns) occurs from thermally relaxed states or even excitonic states of the perovskite near the band edge, not representative of the free carriers typically generated in the $CH_3NH_3PbI_3$ material with higher excitation energy. To investigate if there is a dependence

DOI: 10.1021/acs.jpclett.5b01698
J. Phys. Chem. Lett. 2015, 6, 3675−3681

of the slow hole transfer on the excess energy of the absorbed photons, we repeated the experiment on the same samples with an excitation wavelength of 580 nm. The results are summarized in Figure 3.

At 580 nm, we excited transitions in the perovskite as well as in the P3HT, especially because we irradiated from the P3HT side. Therefore, immediately after excitation, the TAS spectra contain signatures of the GSB of P3HT as well as bands related to the excited perovskite (clearly visible at 1 ps in Figure 3A). The polymer's GSB increases with HTM thickness, due to enhanced direct excitation of the P3HT. For the thicker P3HT layer (135 nm), there is a strong filtering effect, with most of the photons being absorbed within the P3HT layer, so that the amplitude of the 760 nm band of $CH_3NH_3PbI_3$ is strongly reduced. As with the data shown in Figure 1A, in the case of the $TiO_2/CH_3NH_3PbI_3$ film measured for the new set of experiments, the dynamics can be globally reproduced by the sum of three exponential functions, having a subpicosecond component, a weak component of about 100 ps and a slow component exceeding the measurement window. Because the subpicosecond component is strongly reduced when exciting at 760 nm close to the band gap of the perovskite, it is related to the thermal relaxation of hot electrons and holes. The 100 ps components might be related to the formation of excitons[22] and the slow component is related to the lifetime of the excited state.

In Figure 3B, the dynamics at 620 nm upon excitation at 580 nm are compared for the $TiO_2/CH_3NH_3PbI_3$ reference sample for the sample with a medium thickness of P3HT (45 nm) and with a thicker P3HT layer (135 nm). At this wavelength, the GSB of the P3HT, the PIA of the perovskite and some early relaxation dynamics in the perovskite are simultaneously probed. Thus, the signals reflect the processes happening in the bulk perovskite, interfacial processes between (photoexcited) P3HT and (photoexcited) perovskite, and processes within bulk P3HT. With the thickest P3HT layer, the signal is dominated by the GSB of the polymer, which decays to zero on a time scale comparable to what has been reported for neat P3HT films.[26] Mainly, the dynamics of excitons within bulk P3HT, which hardly interact with the perovskite interface, are seen. On the other hand, the negative GSB of P3HT in the sample with the intermediate P3HT layer (45 nm) is replaced by the positive signal of the perovskite PIA within a few picoseconds. We ascribe this to quenching of interfacial P3HT excitons by energy transfer to $CH_3NH_3PbI_3$. This attribution is supported by the comparison of back and front side excitation of the sample (see Supporting Information Figure S6). The signature of the P3HT ground state bleaching at 620 nm completely vanishes shortly after excitation due to energy transfer to perovskite, leaving only signatures of excited perovskite having the same amplitude for front and backside excitation. This means that any excitation energy from direct P3HT excitation on the P3HT side has been transferred to the perovskite. Only at much longer times, the ingrowth of the P3HT GSB signal occurs with the same rate constant for both excitation directions, due to slow hole transfer to P3HT. At longer time scales, the signal at 620 nm decays faster than in the reference sample without HTM. Inspection of the normalized TA spectra in Figure 3C indicates that this encompasses a slow increase in relative amplitude of the GSB of P3HT, as expected for slow hole transfer at the interface. Slow hole transfer thus also occurs with 580 nm excess energy excitation of the perovskite. Overall, the dynamics in this sample strongly confirm what was observed for the thinnest (5−10 nm) P3HT layer in Figure 1.

Global analysis was carried out on the data obtained upon excitation at 580 nm. When the P3HT layer is added, at least five exponential functions are necessary to reproduce the TAS data (Figure 3D−F). As for the $TiO_2/CH_3NH_3PbI_3$ reference sample, there is a subpicosecond relaxation component encompassing GSB and SE of the perovskite, but also GSB and SE of the P3HT at around 620 and 690 nm, respectively. For the thickest (135 nm) P3HT layer, the dynamics are dominated by processes in bulk P3HT. Here, we find two further components associated with a decay of the GSB of P3HT, correlated to SE bands at 700 and 710 nm and time constants of 4.5 and 103 ps, respectively. The progressive red-shift of the SE band of P3HT (with the subps and 4.5 ps time constants) is similar to what has been observed in neat P3HT films, and the longer 103 ps time constant corresponds to the decay of the excited state in P3HT.[26] On a longer time scale, τ = 2334 ps, we observe a weak increase of the GSB of P3HT, indicating hole transfer from the perovskite to P3HT. The 7 ns component contains features of excited $CH_3NH_3PbI_3$ as well as the GSB of P3HT. Because a large fraction of excitons decays within the P3HT layer without generating charges, this layer is evidently too thick for any solar cell applications.

For the reduced P3HT layer thickness (45 nm), the subpicosecond relaxation remains the same, but the initial decay of the GSB of P3HT now occurs almost monoexponentially with a time constant of τ = 15 ps, and the P3HT exciton decay component at around 100 ps almost vanishes. The ratio of the amplitudes associated with the GSB (620 nm) and the SE (∼700 nm) is 2 and 5 for the thicker and thinner P3HT layer, respectively. The decrease of the emission in 15 ps as well as the missing 100 ps component suggest a different decay pathway in the 45 nm P3HT sample, which we attribute to energy transfer from excited P3HT to the perovskite. The third process, a growth of the GSB of P3HT due to the previously described hole transfer reaction, occurs again with a 2333 ps time constant, and is independent of whether the sample is excited from the P3HT or $CH_3NH_3PbI_3$ side (this mainly affects the extent of direct P3HT excitation, Supporting Information Figure S6). The time scale of the hole transfer reaction is similar to the one observed upon 760 nm excitation. Therefore, we conclude that the slow hole transfer dynamics observed in perovskite/P3HT systems is not due to band-edge excitation performed at 760 nm excitation wavelength. Moreover, we can conclude that the hole transfer reaction occurs from thermally relaxed states because the dynamics are similar for both excitation energies and thermal relaxation has been observed to occur on a subpicosecond time scale.

It is interesting to note that the hole transfer from photoexcited $CH_3NH_3PbI_3$ to P3HT is about 4 orders of magnitude slower compared to the previously published hole transfer time to Spiro-OMeTAD.[15,22] The similar quenching rate of the transient signals at 500 and 755 nm, see Figure 1C, suggests that the hole transfer from photoexcited Perovskite to the HTM occurs on a comparable rate for PCPDTBT, PTAA, and P3HT. The onsets of the oxidation potentials for P3HT, PCPDTBT, PTAA, and Spiro-OMeTAD, −5.1 eV, −5.3 eV, −5.2 eV, and −5.22 eV respectively,[8] are rather similar, suggesting similar driving forces for the hole transfer reactions due to similar band-alignment. Slower hole transfer might be related to a reduced physical contact between the perovskite and P3HT due incomplete infiltration of the mp-TiO_2/

DOI: 10.1021/acs.jpclett.5b01698
J. Phys. Chem. Lett. 2015, 6, 3675−3681

$CH_3NH_3PbI_3$ layer. Less physical contact, due to the roughness of the TiO_2/perovskite layer, would increase the need for diffusion of the charges before finding a suitable site for charge transfer. SEM images of $TiO_2/CH_3NH_3PbI_3$ and $TiO_2/CH_3NH_3PbI_3$/P3HT samples are shown in Supporting Information Figure S7. Although the capping layer of P3HT is clearly visible (Supporting Information Figure S7C), it seems that infiltration deeper in the film is incomplete, leading to regions with a poor P3HT/$CH_3NH_3PbI_3$ contact. Another possible explanation would be a reduced electronic coupling of P3HT to $CH_3NH_3PbI_3$, but it seems to be improbable because Bi et al. measured electron lifetime in perovskite/Spiro-OMeTAD and perovskite/P3HT systems and attributed the longer electron lifetime in perovskite/Spiro-OMeTAD to worse coupling due to the spiro shape.[28]

In conclusion, we have shown that hole transfer from photoexcited $CH_3NH_3PbI_3$ to P3HT occurs on a time scale of a few nanoseconds and from the thermally relaxed perovskite. The rate of hole transfer was found to be independent of excess excitation energy. Moreover, excitons in P3HT undergo rapid quenching if they are generated near the perovskite/P3HT interface. The quenching is likely attributed to energy transfer from the photoexcited P3HT to $CH_3NH_3PbI_3$. Because the excitons have to reach the interface prior to the energy transfer, the optimal thickness of the P3HT layer should not exceed the exciton diffusion length in P3HT. This mechanism provides the possibility of sensitizing perovskites and harvesting photons absorbed by the HTM. On the other hand, owing to the long lifetime and diffusion length of charges in $CH_3NH_3PbI_3$[6,14,29] the relatively slow hole transfer rate to the P3HT layer does not present a major drawback. It might even be prevented by an optimized design, increasing the interfacial contact area.

■ ASSOCIATED CONTENT

Supporting Information

The Supporting Information is available free of charge on the ACS Publications website at DOI: 10.1021/acs.jpclett.5b01698.

Sample preparation details as well as the experimental setup and data-analysis are described in Supporting Information together with supporting data. (PDF)

■ AUTHOR INFORMATION

Corresponding Author

*E-mail: Natalie.banerji@unifr.ch.

Notes

The authors declare no competing financial interest.

■ ACKNOWLEDGMENTS

The Authors thank Jingshan Luo (EPFL) for taking the SEM images. N.B. and J.B. thank the Swiss National Science Foundation (PP00P2_150536) and the university of Fribourg for funding, as well as Prof. J.-E. Moser (EPFL) and Dr. A. Marchioro for useful discussions. Y.H.L. and M.K.N. acknowledge funding from the European Union Seventh Framework Program [FP7/2007-2013] under grant agreement no. 604032 of the MESO project, (FP7/2007-2013) ENERGY.2012.10.2.1; NANOMATCELL, grant agreement no. 308997.

■ REFERENCES

(1) Burschka, J.; Pellet, N.; Moon, S. J.; Humphry-Baker, R.; Gao, P.; Nazeeruddin, M. K.; Gratzel, M. Sequential Deposition as a Route to High-Performance Perovskite-Sensitized Solar cells. *Nature* **2013**, *499*, 316−319.

(2) Sum, T. C.; Mathews, N. Advancements in Perovskite Solar Cells: Photophysics Behind the Photovoltaics. *Energy Environ. Sci.* **2014**, *7*, 2518−2534.

(3) Gratzel, M. The Light and Shade of Perovskite Solar Cells. *Nat. Mater.* **2014**, *13*, 838−842.

(4) Lee, M. M.; Teuscher, J.; Miyasaka, T.; Murakami, T. N.; Snaith, H. J. Efficient Hybrid Solar Cells Based on Meso-Superstructured Organometal Halide Perovskites. *Science* **2012**, *338*, 643−647.

(5) Wehrenfennig, C.; Eperon, G. E.; Johnston, M. B.; Snaith, H. J.; Herz, L. M. High Charge Carrier Mobilities and Lifetimes in Organolead Trihalide Perovskites. *Adv. Mater.* **2014**, *26*, 1584−1589.

(6) Stranks, S. D.; Eperon, G. E.; Grancini, G.; Menelaou, C.; Alcocer, M. J. P.; Leijtens, T.; Herz, L. M.; Petrozza, A.; Snaith, H. J. Electron-Hole Diffusion Lengths Exceeding 1 Micrometer in an Organometal Trihalide Perovskite Absorber. *Science* **2013**, *342*, 341−344.

(7) Eperon, G. E.; Stranks, S. D.; Menelaou, C.; Johnston, M. B.; Herz, L. M.; Snaith, H. J. Formamidinium Lead Trihalide: A Broadly Tunable Perovskite for Efficient Planar Heterojunction Solar Cells. *Energy Environ. Sci.* **2014**, *7*, 982−988.

(8) Cui, J.; Yuan, H.; Li, J.; Xu, X.; Shen, Y.; Lin, H.; Wang, M. Recent Progress in Efficient Hybrid Lead Halide Perovskite Solar Cells. *Sci. Technol. Adv. Mater.* **2015**, *16*, 036004.

(9) Jung, H. S.; Park, N.-G. Perovskite Solar Cells: From Materials to Devices. *Small* **2015**, *11*, 10−25.

(10) Kojima, A.; Teshima, K.; Shirai, Y.; Miyasaka, T. Organometal Halide Perovskites as Visible-Light Sensitizers for Photovoltaic Cells. *J. Am. Chem. Soc.* **2009**, *131*, 6050−6051.

(11) NREL. Best Research Cell Efficiency. http://www.nrel.gov/ncpv/images/efficiency_chart.jpg (accessed August, 2015).

(12) Marchioro, A.; Teuscher, J.; Friedrich, D.; Kunst, M.; van de Krol, R.; Moehl, T.; Gratzel, M.; Moser, J. E. Unravelling the Mechanism of Photoinduced Charge Transfer Processes in Lead Iodide Perovskite Solar Cells. *Nat. Photonics* **2014**, *8*, 250−255.

(13) Ponseca, C. S.; Savenije, T. J.; Abdellah, M.; Zheng, K. B.; Yartsev, A.; Pascher, T.; Harlang, T.; Chabera, P.; Pullerits, T.; Stepanov, A.; et al. Organometal Halide Perovskite Solar Cell Materials Rationalized: Ultrafast Charge Generation, High and Microsecond-Long Balanced Mobilities, and Slow Recombination. *J. Am. Chem. Soc.* **2014**, *136*, 5189−5192.

(14) Xing, G.; Mathews, N.; Sun, S.; Lim, S. S.; Lam, Y. M.; Grätzel, M.; Mhaisalkar, S.; Sum, T. C. Long-Range Balanced Electron- and Hole-Transport Lengths in Organic-Inorganic CH3NH3PbI3. *Science* **2013**, *342*, 344−347.

(15) Kim, H.-S.; Lee, C.-R.; Im, J.-H.; Lee, K.-B.; Moehl, T.; Marchioro, A.; Moon, S.-J.; Humphry-Baker, R.; Yum, J.-H.; Moser. Lead Iodide Perovskite Sensitized All-Solid-State Submicron Thin Film Mesoscopic Solar Cell with Efficiency Exceeding 9%. *Sci. Rep.* **2012**, *2:591*, 591.

(16) Xing, G. C.; Mathews, N.; Sun, S. Y.; Lim, S. S.; Lam, Y. M.; Gratzel, M.; Mhaisalkar, S.; Sum, T. C. Long-Range Balanced Electron- and Hole-Transport Lengths in Organic-Inorganic $CH_3NH_3PbI_3$. *Science* **2013**, *342*, 344−347.

(17) Yan, K.; Wei, Z.; Li, J.; Chen, H.; Yi, Y.; Zheng, X.; Long, X.; Wang, Z.; Wang, J.; Xu.; et al. High-Performance Graphene-Based Hole Conductor-Free Perovskite Solar Cells: Schottky Junction Enhanced Hole Extraction and Electron Blocking. *Small* **2015**, *11*, 2269−2274.

(18) Heo, J. H.; Im, S. H.; Noh, J. H.; Mandal, T. N.; Lim, C. S.; Chang, J. A.; Lee, Y. H.; Kim, H. J.; Sarkar, A.; Nazeeruddin, Md. K.; et al. Efficient Inorganic-Organic Hybrid Heterojunction Solar Cells Containing Perovskite Compound and Polymeric Hole Conductors. *Nat. Photonics* **2013**, *7*, 487−492.

(19) Bi, D.; Moon, S.-J.; Haggman, L.; Boschloo, G.; Yang, L.; Johansson, E. M. J.; Nazeeruddin, M. K.; Gratzel, M.; Hagfeldt, A. Using a Two-Step Deposition Technique to Prepare Perovskite

DOI: 10.1021/acs.jpclett.5b01698
J. Phys. Chem. Lett. 2015, 6, 3675−3681

($CH_3NH_3PbI_3$) for Thin Film Solar Cells Based on ZrO_2 and TiO_2 Mesostructures. *RSC Adv.* **2013**, *3*, 18762−18766.
(20) D'Innocenzo, V.; Grancini, G.; Alcocer, M. J. P.; Kandada, A. R. S.; Stranks, S. D.; Lee, M. M.; Lanzani, G.; Snaith, H. J.; Petrozza, A. Excitons versus Free Charges in Organo-Lead Trihalide Perovskites. *Nat. Commun.* **2014**, *5*, 1−6.
(21) Lin, Q.; Armin, A.; Nagiri, R. C. R.; Burn, P. L.; Meredith, P. Electro-Optics of Perovskite Solar Cells. *Nat. Photonics* **2014**, *9*, 106−112.
(22) Piatkowski, P.; Cohen, B.; Javier Ramos, F.; Di Nunzio, M.; Nazeeruddin, M. K.; Gratzel, M.; Ahmad, S.; Douhal, A. Direct Monitoring of Ultrafast Electron and Hole Dynamics in Perovskite Solar Cells. *Phys. Chem. Chem. Phys.* **2015**, *17*, 14674−14684.
(23) Stamplecoskie, K. G.; Manser, J. S.; Kamat, P. V. Dual Nature of the Excited State in Organic-Inorganic Lead Halide Perovskites. *Energy Environ. Sci.* **2015**, *8*, 208−215.
(24) Manser, J. S.; Kamat, P. V. Band Filling with Free Charge Carriers in Organometal Halide Perovskites. *Nat. Photonics* **2014**, *8*, 737−743.
(25) Hsu, H.-Y.; Wang, C.-Y.; Fathi, A.; Shiu, J.-W.; Chung, C.-C.; Shen, P.-S.; Guo, T.-F.; Chen, P.; Lee, Y.-P.; Diau, E. W.-G. Femtosecond Excitonic Relaxation Dynamics of Perovskite on Mesoporous Films of Al_2O_3 and NiO Nanoparticles. *Angew. Chem., Int. Ed.* **2014**, *53*, 9339−9342.
(26) Banerji, N.; Cowan, S.; Vauthey, E.; Heeger, A. J. Ultrafast Relaxation of the Poly(3-hexylthiophene) Emission Spectrum. *J. Phys. Chem. C* **2011**, *115*, 9726−9739.
(27) van Stokkum, I. H. M.; Larsen, D. S.; van Grondelle, R. Global and Target Analysis of Time-Resolved Spectra. *Biochim. Biophys. Acta, Bioenerg.* **2004**, *1657*, 82−104.
(28) Bi, D. Q.; Yang, L.; Boschloo, G.; Hagfeldt, A.; Johansson, E. M. J. Effect of Different Hole Transport Materials on Recombination in $CH_3NH_3PbI_3$ Perovskite-Sensitized Mesoscopic Solar Cells. *J. Phys. Chem. Lett.* **2013**, *4*, 1532−1536.
(29) Dong, Q.; Fang, Y.; Shao, Y.; Mulligan, P.; Qiu, J.; Cao, L.; Huang, J. Electron-Hole Diffusion Lengths > 175 μm in Solution-Grown $CH_3NH_3PbI_3$ Single Crystals. *Science* **2015**, *347*, 967−970.

DOI: 10.1021/acs.jpclett.5b01698
J. Phys. Chem. Lett. 2015, 6, 3675−3681